JOURNAL OF MATERIALS SCIENCE 17 (1982) 3347–3360

Diffusion bonding stainless steel to alumina using aluminium interlayers

M. G. NICHOLAS, R. M. CRISPIN
Materials Development Division, AERE Harwell, Didcot, Oxfordshire, UK

A study has been conducted to identify the effects of fabrication temperatures pressures, times and other variables on the strengths of diffusion-bonded joints between alumina and BS321 stainless steel produced using aluminium foil interlayers. The strengths of the alumina–aluminium and steel–aluminium interfaces were found to be influenced differently by some fabrication parameters, thus increasing the fabrication temperature promoted alumina–aluminium bonding but also accelerated the growth of ultimately weakening intermetallic layers at steel–aluminium interfaces. It was concluded that the optimum conditions for bonding BS321 stainless steel to alumina could be achieved by using a 0.5 mm aluminium foil, applying a 50 MPa pressure for 30 min in an evacuated chamber at 625° C. In discussing the results of this study, attention is paid to the problems or advantages of using foils and metal components other than aluminium or BS321 steel and particular note is taken of thermal expansion mismatch effects.

1. Introduction

The achievement of high-integrity ceramic–metal joints required for engineering devices such as electrical feed-throughs is not easy and has led to the development of a range of special fabrication techniques. One of the most recent of these is diffusion bonding in which pressures and high temperatures are used to bring ceramic and metal members into such intimate contact that interfacial adhesion is produced by virtue of forces that act on an atomic scale.

Various metals and alloys have been diffusion bonded to ceramics but practical difficulties can be caused during the application of the process to component manufacture. In particular, problems can be caused by the need to deform the metal and the stressing of the joint by thermal contraction mismatch stresses generated as the bonded component cools. It has been found that the use of a soft material layer inserted between the ceramic and metal members can overcome or mitigate the effects of some of these practical problems. However, this practice can also make it difficult to predict the optimum fabrication conditions since the effects of variations may differ for the ceramic–metal and metal–metal interfaces, particularly if brittle intermetallic compounds are formed at the metal–intermediate layer interface.

In view of these difficulties, the work described in this paper was undertaken in an attempt to provide information about the optimum conditions for fabricating intermediate layer diffusion-bonded joints. Specifically, the study was concerned with the bond strengths of BS321 stainless steel–aluminium–alumina joints which could find applications in vacuum and electrical components. Attention was paid to the effects of varying individual fabrication parameters such as temperature, time and pressure.

2. Materials and techniques

A variety of materials and techniques were used in the work, but attention will be focused on those employed during the main series of experiments. The ceramic used in these was 97.5% pure Deranox alumina supplied by Anderman and Ryder Ltd, in the form of ASTM test pieces, as sketched in Fig. 1. Pairs of these test pieces were bonded to 10 mm high, 16 mm o.d., 7 mm i.d. samples of BS321, 18/9/1 CrNiTi steel, whose nominal composition is given in Table I, via aluminium annuli,

0022–2461/82/113347–14$04.18/0

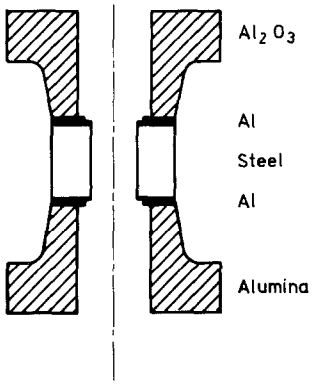

Figure 1 ASTM bonded ceramic test pieces according to designation F19-64.

usually 0.5 mm thick, cut from commercial purity foil.

Care was taken not to touch the bonding surfaces of the alumina test pieces, which were used in the as-received, fired condition. The bonding surfaces of the aluminium foils and stainless steel samples, however, were roughened using alumina abrasive cloth and ultrasonically degreased in Genklene for 5 min. In this condition, the metal surfaces were slightly contaminated by organic materials identified by infrared spectroscopy as alkyl phthalate esters, an impurity in the Genklene, but heating in a vacuum or air to temperatures above 350° C removed this unwanted material. Profilometry data for the various materials are presented in Table II.

The samples were assembled and lightly clamped together before being introduced into the hot-pressing facility sketched in Fig. 2. Usually, the hot-pressing chamber was evacuated to a few mPa before the samples were heated to the bonding temperature, which ranged from 496 to 625° C. The heat-up time was 2 to 3 h, after which the samples were subjected to a compressive stress of 25 to 100 MPa (load divided by the bonding surface area of the ASTM test pieces) and held at temperature for 10 to 120 min. At the end of this time, the power supply to the chamber heater was switched off and the pressure released. The samples were allowed to cool slowly, not being unloaded until 16 h had elapsed.

TABLE I Composition of the alloys used in this work

BS321
17.1 Cr, 9.0 Ni, 1.57 Mn, 0.65 Mo, 0.33 Si, 0.28 Cu, 0.26 Ti, 0.23 Co, 0.041 P, 0.025 N, 0.024 C, 0.023 S, remainder Fe.

BS431
16.1 Cr, 2.1 Ni, 0.12 C, remainder Fe.

BS310
24.5 Cr, 20.5 Ni, 0.15 C, remainder Fe.

Inconel 600
15.8 Cr, 7.2 Fe, 0.04 C, remainder Ni.

Invar
36.1 Ni, 0.5 Mn, 0.2 Si, 0.1 C, remainder Fe.

Many experiments were conducted using the materials and procedures described above, but major variations were introduced in three short series. When bonding was attempted using argon atmospheres, the hot pressing chamber was evacuated before being backfilled with sufficient 99.998% pure argon to produce a pressure of just less than 1 atm at the bonding temperature. Truncated cone ceramic samples manufactured from 97.6% pure alumina, UL 300, by English Glass Ltd, were bonded via aluminium foils to discs of copper, iron, platinum, titanium or type BS 316 stainless steel as indicated in Fig. 3. Finally, several experiments were performed in which various metals or alloys were bonded together using aluminium foils.

The quality of bonded samples was assessed primarily by tensile tests conducted at an extension rate of 1 mm min^{-1} using an Instron 1195 machine. The simple parameter of failure load divided by the test piece bonding surface area was used to characterize strengths since the load–extension curves generated for each sample showed that fracture preceded yielding. For some samples, this simple evaluation of quality was supplemented by optical microscopy and electron probe microanalysis of polished cross-sections.

3. Experimental results

3.1. Main series – ASTM test pieces

After the first few experiments, the normal bonding conditions were defined as a pressure of 50 MPa applied for 30 min to a sample held in a vacuum of a few mPa at 590 to 600° C. In subsequent series of experiments individual fabrication parameters were varied while the others were not knowingly allowed to deviate from the norm.

Normal bonding conditions squashed the aluminium foils from 0.5 to 0.165 mm and produced samples that could withstand tensile stresses of 29.5 ± 2.2 MPa before fracturing at

TABLE II Bonding-surface roughness parameters as defined by surface profilometry

Parameter	Alumina	Al	BS321
Average roughness, Ra (μm)	0.50 ± 0.07	1.76 ± 0.23	0.43 ± 0.015
Skewness	−0.98 ± 0.31	+0.02 ± 0.41	−0.28 ± 0.14
Peak to valley height (μm)	3.73 ± 1.21	9.3 ± 1.2	2.43 ± 0.27
Wavelength (μm)	46.94 ± 3.14	98.72 ± 23.7	44.16 ± 1.48
Mean slope (deg)	3.85 ± 0.13	6.62 ± 0.20	3.45 ± 0.15

their alumina– aluminium interfaces. Intermetallic layers about 12 μm thick were present at the unbroken steel–aluminium interfaces as illustrated in Fig. 4. Electron probe microanalyser surveys of these layers revealed two zones; an approximately 2 μm thick inner layer adjacent to the steel with a composition corresponding to $(Fe_{0.70}Cr_{0.18}Ni_{0.08}Mn_{0.02}Si_{0.02})Al_{2.60}$ and an outer thicker layer of $(Fe_{0.68}Cr_{0.18}Ni_{0.08}Mn_{0.01}Si_{0.05})Al_{3.26}$.

When non-standard bonding conditions were used, the sample strengths and intermetallic thicknesses varied considerably as shown by the data, derived in general from duplicated or triplicated experiments, listed in Table III. The influence of individual fabrication parameters on bond strength values and steel–aluminium interaction layer thicknesses are illustrated in Figs 5 to 12 and the principal observations are summarized below.

3.1.1. Temperature

Increasing the fabrication temperature from 496 to 625° C caused the joints to become progressively stronger, those formed at 496, 542 and 594° C ultimately failing at alumina–aluminium interfaces and those formed at 625° C failing at steel–aluminium interfaces (Fig. 5). The influence of fabrication temperature on strengths of joints failing at alumina–aluminium interfaces can be described by an expression of the type:

$$BS = B_0 e^{-QB/RT} \quad (1)$$

where BS is the bond strength in MPa, B_0 a constant with a value of 3.14×10^6 MPa, QB is an apparent activation energy with a value of 83.3 kJ mol^{-1}, R is the gas constant, and T the temperature in K. The expression predicts that the alumina–aluminium interfaces of samples

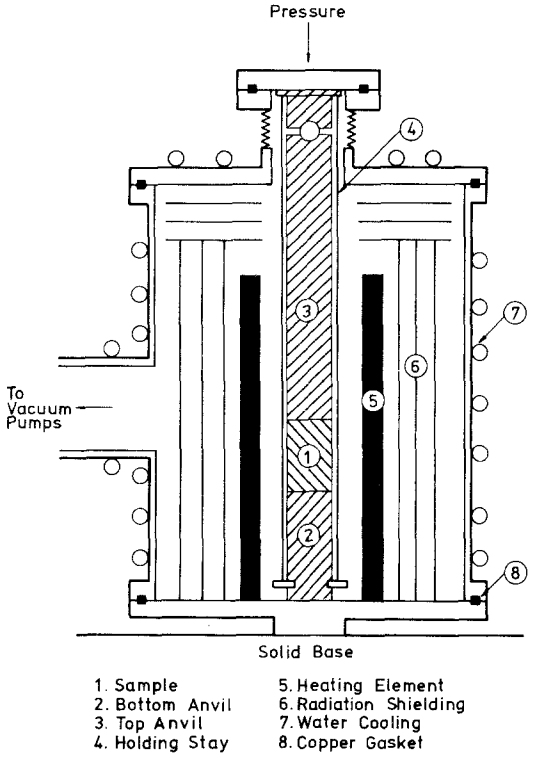

Figure 2 Schematic diagram of the vacuum hot-pressing facility.

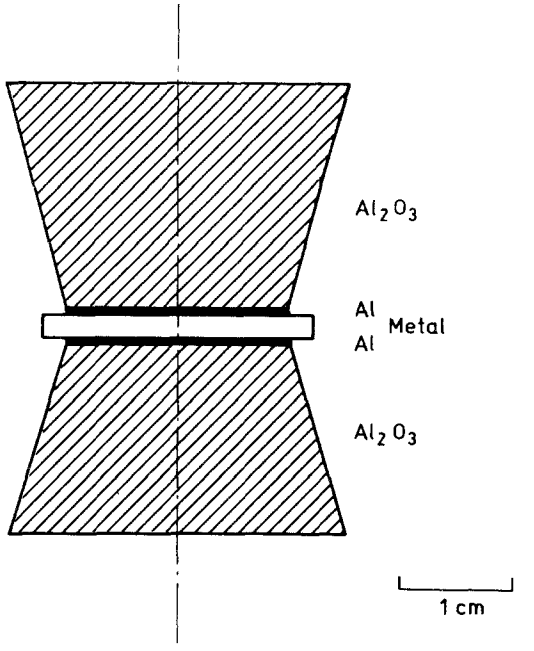

Figure 3 Truncated cone bond-strength test pieces.

TABLE III Main series experimental data

Temperature (°C)	Pressure (mPa)	Time (min)	Environment	Surface preparation	Post-fabrication heat treatment	Interlayer thickness		Strength (MPa)	Fracture location*	Intermetallic thickness (μm)
						Original (mm)	Final (mm)			
496	50	30	Vacuum	Abraded	None	0.5	0.165 ± 0.01	6.8 ± 1.5	A	1 ± 0.5
542	50	30	Vacuum	Abraded	None	0.5	0.165 ± 0.01	15.1 ± 2.0	A	2 ± 0.5
594	50	30	Vacuum	Abraded	None	0.5	0.165 ± 0.01	29.5 ± 2.2	A	12.8 ± 1.9
625	50	30	Vacuum	Abraded	None	0.5	0.165 ± 0.01	41.5 ± 1.3	S	18.8 ± 2.3
587	50	10	Vacuum	Abraded	None	0.5	0.165 ± 0.01	14.6 ± 4.3	A	8.3 ± 1.0
595	50	60	Vacuum	Abraded	None	0.5	0.165 ± 0.01	30.5 ± 3.7	A	15.2 ± 1.7
597	50	120	Vacuum	Abraded	None	0.5	0.165 ± 0.01	27.7 ± 6.8	S	20 ± 1.0
591	25	30	Vacuum	Abraded	None	0.5	0.165 ± 0.01	14.2 ± 0.1	A	12.5 ± 1.0
595	100	30	Vacuum	Abraded	None	0.5	0.165 ± 0.01	27.3 ± 3.1	S	12.0 ± 0.5
600	50	30	Vacuum	Abraded	None	1.0	0.170 ± 0.005	39.6 ± 6.9	S	13.5 ± 1.0
601	50	30	Vacuum	Abraded	None	0.2	0.146 ± 0.01	25.8 ± 4.7	A	13.0 ± 3.1
601	50	30	Vacuum	Abraded	None	0.1	0.075 ± 0.005	27.6 ± 2.4	A	12.5 ± 0.5
595	50	30	Argon	Abraded	None	0.5	0.165 ± 0.01	17.1 ± 1.7	S	4.2 ± 0.5
602	50	30	Air	Abraded	None	0.5	0.165 ± 0.01	3.8 ± 1.4	S	2.1 ± 0.5
493	50	30	Air	Abraded	None	0.5	0.165 ± 0.01	7.2 ± 0.9	A	1.0 ± 1.0
600	50	30	Vacuum	Abraded	16 h at 75° C	0.5	0.165 ± 0.01	27.2	A	14.6 ± 0.5
601	50	30	Vacuum	Abraded	16 h at 100° C	0.5	0.165 ± 0.01	74.4	S	16.7 ± 1.0
594	50	30	Vacuum	Abraded	16 h at 125° C	0.5	0.165 ± 0.01	50.4	A	14.8 ± 0.5
599	50	30	Vacuum	Abraded	16 h at 150° C	0.5	0.165 ± 0.01	52	A	15.8 ± 1.3
602	50	30	Vacuum	Abraded	16 h at 175° C	0.5	0.165 ± 0.01	35.2	A	15.7 ± 1.1
596	50	30	Vacuum	Abraded	16 h at 200° C	0.5	0.165 ± 0.01	16.3	A	14.3 ± 0.5
601	50	30	Vacuum	Abraded	16 h at 300° C	0.5	0.165 ± 0.01	15	A	16.5 ± 1.4

*A, alumina–aluminium interface; S, steel–aluminium interface.

Figure 4 Intermetallic layers present at a steel–aluminium interface bonded for 30 min at 594° C, × 480.

fabricated at 625° C would have failed at a stress of 45 MPa, as opposed to the 41.5 ± 1.3 MPa at which their steel–aluminium interfaces actually failed.

Failure of samples produced at 625° C occurred through a 19 μm thick intermetallic layer but layers present in samples that failed at their alumina–aluminium interfaces were thinner, as shown in Fig. 6. The thicknesses of layers formed during a 30 min pressing could be related to the fabrication temperature by an expression of the form

$$X = A\,e^{-B/T} \qquad (2)$$

where X is the layer thickness and A and B are constants with values of $5.44 \times 10^{10}\,\mu$m and 19 325 K.

3.1.2. Time

Changing the fabrication times of samples produced at about 587 to 597° C from 30 to 10 or 120 min caused them to fail at steel–aluminium rather than alumina–aluminium interfaces. The use of short fabrication times weakened the samples, but increasing the time had no significant effect on joint strengths as shown in Fig. 7.

The thickness of the intermetallic layers formed at the steel–aluminium interfaces increased with fabrication time, and Fig. 8 shows that there was a linear dependence between the times and the squares of the thicknesses of layers formed at about 590° C. The data plot suggests that layers about 5 μm thick would have grown as samples cooled after an instantaneous pressing at about 590° C and that layer growth was diffusion controlled. Approximate values of the rate constants for such growth were calculated for several fabrication temperatures from the data plotted in Figs 6 and 8 by assuming a parabolic dependence of thickness on time. The linearity of the data plot in Fig. 9 shows that the fabrication temperatures can be related by a simple Arrhenius expression to these growth constants, and also of others

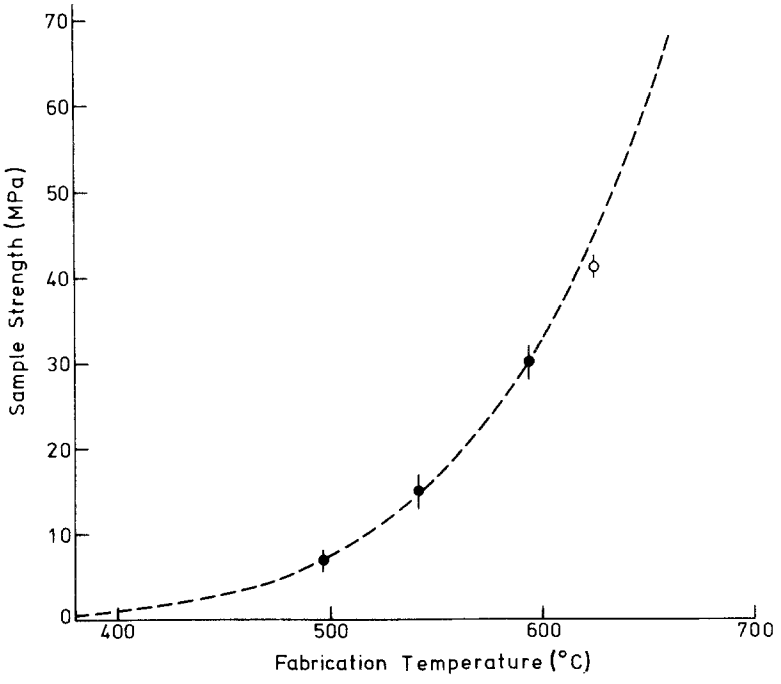

Figure 5 Strengths of samples bonded for 30 min at various temperatures. Solid symbols identify samples that failed at alumina–aluminium interfaces. The dotted line was calculated using Equation 1.

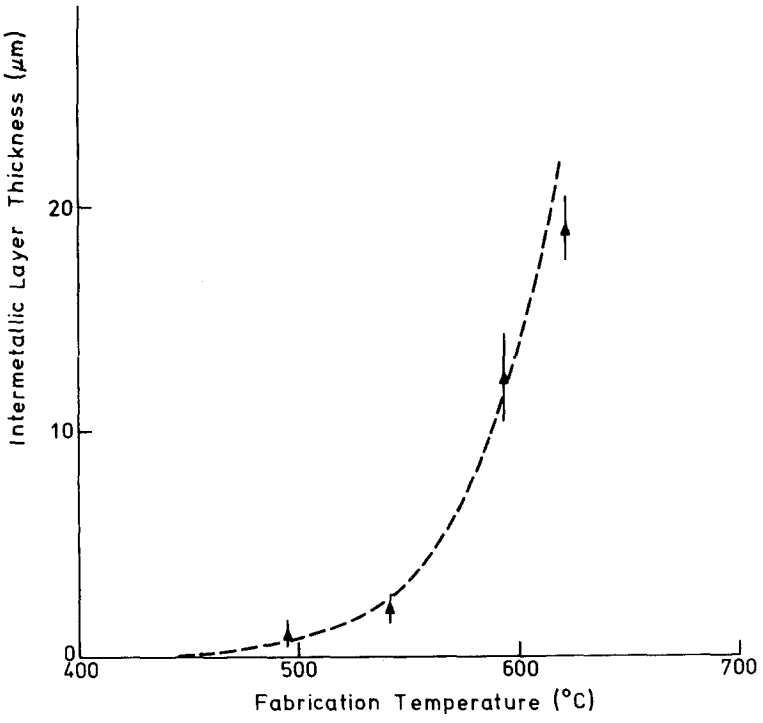

Figure 6 Thicknesses of the intermetallic layers formed at the steel–aluminium interfaces of samples bonded for 30 min at various temperatures. The dotted line was calculated from Equation 2.

derived from the work of Steinleitner [1], who diffusion bonded a similar steel to aluminium, and from earlier work at Harwell in which the 18/9/1 CrNiTi steel was exposed to molten aluminium [2]. The good agreement of these sets of data suggests that the same controlling process was operative and manipulation of the data plot in Fig. 9 permits Equation (2) to be rewritten as

$$X^2 = At\,e^{-Qx/RT} \qquad (3)$$

where A is a constant of value 1.5 $m^2 sec^{-1}$, t is the fabrication time (sec), and Qx is an activation energy of 227 kJ mol^{-1}.

3.1.3. Pressure

Halving the normal pressure used to fabricate the samples decreased their joint strength, failures occurring at their alumina–aluminium interfaces at tensile stresses of 14 MPa. Doubling the applied pressure to 100 mPa strengthened the alumina–aluminium interfaces somewhat so that failures occurred at the steel–aluminium interfaces at stresses of 27 MPa. This change in fracture location was not associated with any thickening of the intermetallic layers formed at the steel–aluminium interfaces.

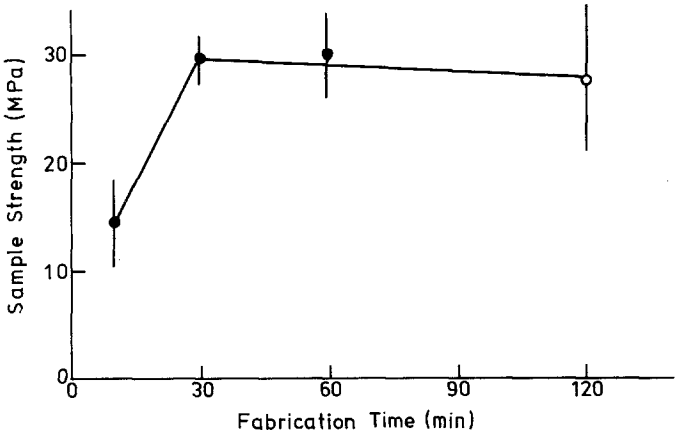

Figure 7 Strengths of samples bonded for various times at 590 to 600° C. Solid symbols identify samples that failed at alumina–aluminium interfaces.

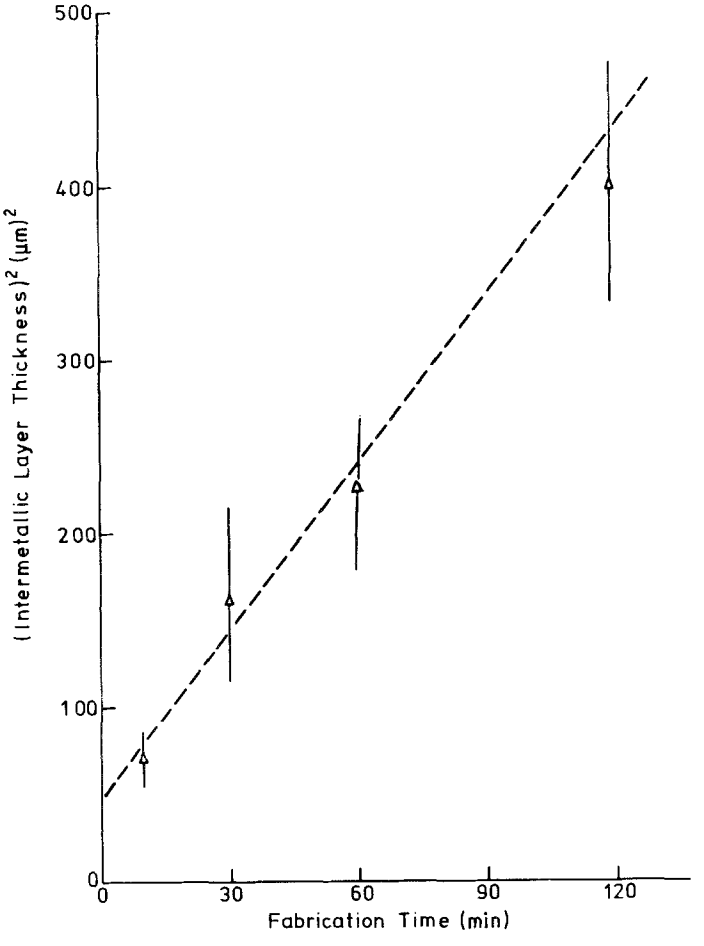

Figure 8 The thicknesses of the intermetallic layers formed at the steel–aluminium interfaces of samples bonded for various times at 587 to 597° C.

3.1.4. Foil thickness

Decreasing the foil thickness from 0.5 to 0.1 mm had little effect on the strengths of the samples, failures occurring at their alumina–aluminium interfaces at stresses within the range 25 to 30 MPa. Similarly, there was no marked effect on the thicknesses of the intermetallic layers formed at the steel–aluminium interfaces. While an increase in the gauge of the foil to 1.0 mm did not alter the thickness of the intermetallic layer, it strengthened the samples, failures ultimately occurring at those steel–aluminium interfaces at stresses of about 40 MPa, as shown in Fig. 10.

Varying the foil thickness had significant effects on the actual fabrication process. Decreasing their thicknesses made it increasingly difficult to abrade the foils satisfactorily without rumpling, but increasing their thicknesses enhanced the extent to which they were squashed and squeezed out from the compressed samples (Fig. 10). The flashes produced with the thickest, 1.0 mm, foils were excessive and the dimensional changes during pressing called for special care during prejigging.

3.1.5. Environment

Modifying the normal bonding practice by refilling the chamber with argon containing about 20 ppm oxygen detrimentally affected the bonding characteristics of the samples. The thicknesses of the intermetallic layers formed at the steel–aluminium interfaces were only about 4 μm as compared to the normal 12 μm and these interfaces failed at stresses of 17 MPa whereas they could normally withstand about 30 MPa.

Even more dramatic effects were exhibited when samples were bonded in air at about 590° C, the intermetallic layer thicknesses decreasing to about 2 μm and the strengths of the steel–aluminium interfaces to a mere 4 MPa. However, there was no significant difference between the extents of steel–aluminium interaction or strengths of samples bonded in air or vacuum at about 490° C.

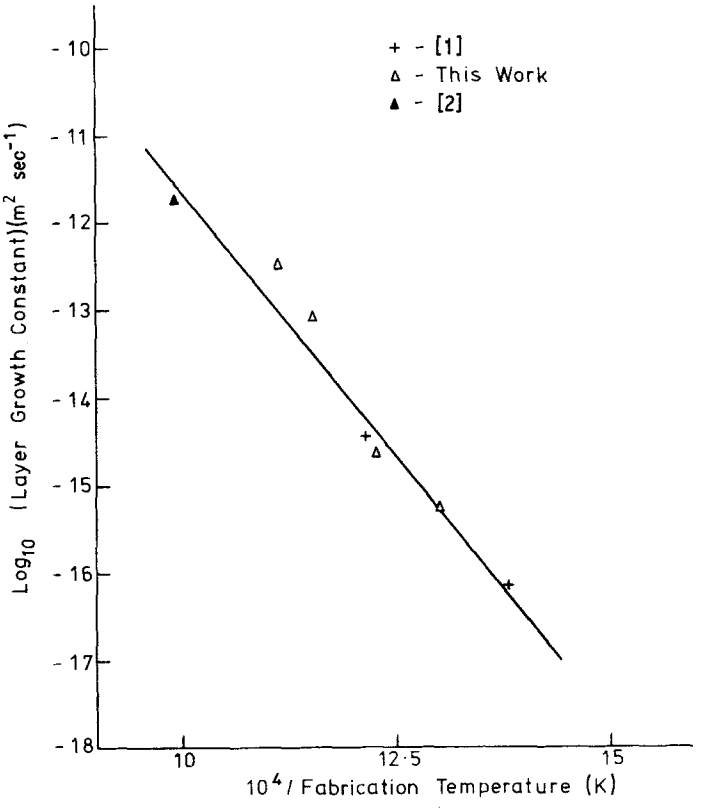

Figure 9 The influence of temperature on the growth constants for intermetallic layers formed at steel–aluminium interfaces.

3.1.6. Post-fabrication heat-treatment

The strengths of bonded samples could be increased by overnight heat treatments at low temperatures, a strength of about 75 MPa being achieved when a temperature of 100° C was used as shown in Fig. 11. The samples that received the most beneficial heat treatment ultimately failed at their steel–aluminium interfaces although there was no clear evidence of changes in the thickness or morphologies of their intermetallic layers.

3.2. Other series

3.2.1. Alumina–aluminium bond studies

Strength data for alumina–aluminium interfaces not subject to steel–alumina thermal expansion mismatch stresses were obtained by testing samples in which ASTM test pieces were bonded directly via 0.5 mm aluminium foils. Both vacuum and argon were used as the chamber environments. There was reasonable agreement between both sets of results and with the work of Dawihl and Klinger [3] who used similar fabrication and testing techniques (Fig. 12). The dependence of these alumina–aluminium interfacial strength values on the fabrication temperature can be

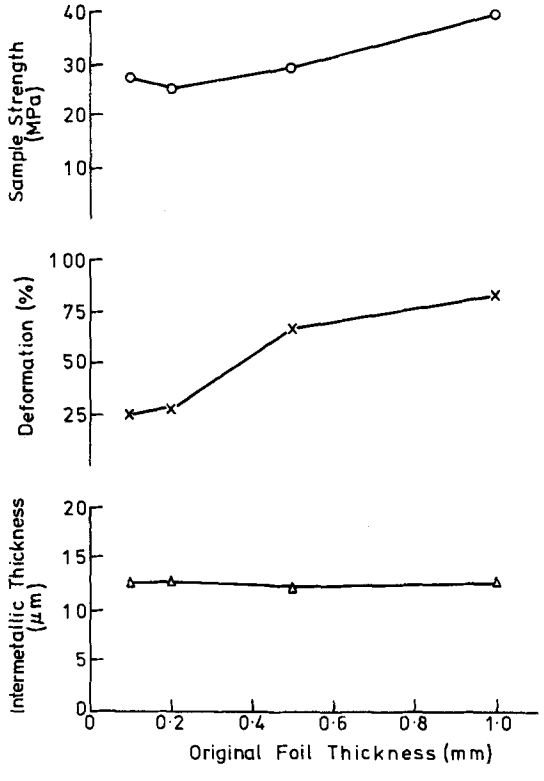

Figure 10 The influence of aluminium foil thickness on some pressing and bonded sample characteristics.

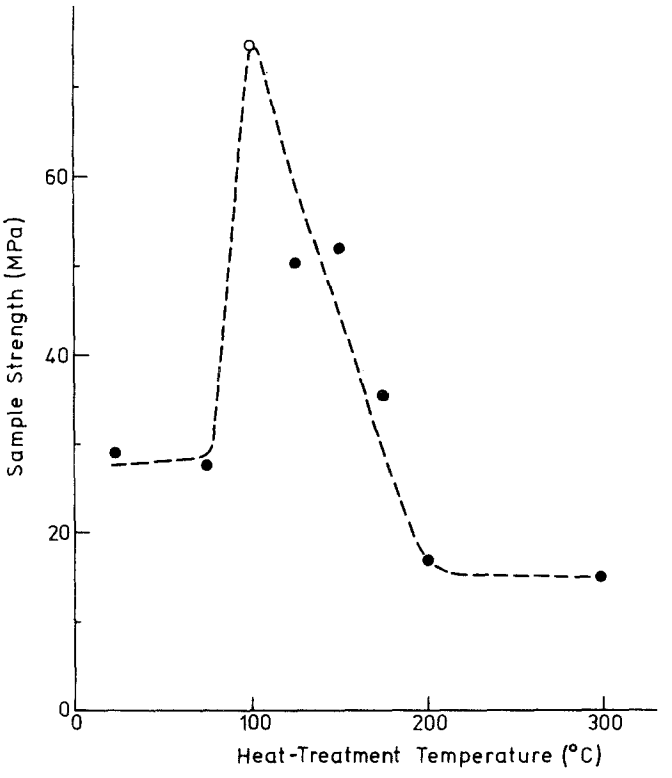

Figure 11 The influence of post-fabrication heat-treatment temperatures on the strengths of samples bonded at 594 to 602° C. Solid symbols identify samples that failed at alumina–aluminium interfaces.

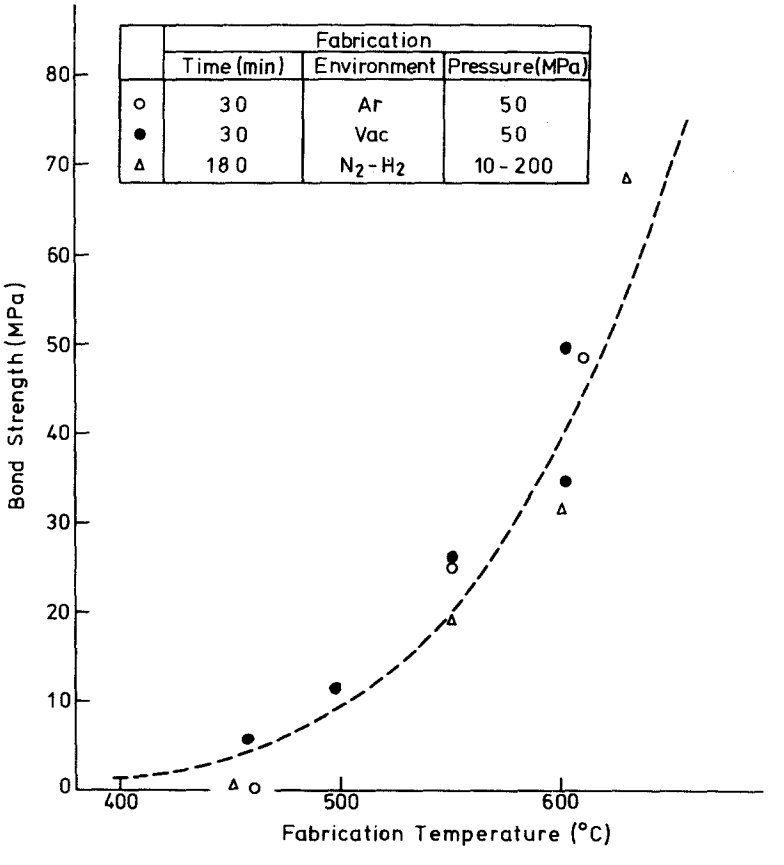

Figure 12 The influence of fabrication temperature on the strength of alumina–aluminium bonds. The dotted line was calculated from the equation $BS = 2.5 \times 10^6 \exp(-80\,300/RT)$ MPa.

represented by an expression such as Equation 1 where B_0 is 2.5×10^6 MPa and QB is 80.3 kJ mol^{-1} as opposed to the 3.14×10^6 MPa and 83.3 kJ mol^{-1} deduced during the main series of experiments.

3.2.2. Thermal expansion mismatch effects

The detrimental effects of mismatches between the thermal expansion coefficient of alumina and that of the metal component to which it is bonded is illustrated by the results of a series of experiments conducted using truncated cone alumina samples. These samples were bonded to 3 mm thick discs of steel, copper and other metals using 1 mm thick foil interlayers. Bonding was produced using pressures of 50 MPa applied for 30 min at 550° C in an argon-filled chamber. The room-temperature strengths of these samples, which all failed at their alumina–aluminium interfaces, varied considerably and could be related to the coefficients of thermal expansion of the metals as shown in Fig. 13, decreasing steadily as they exceeded the 7×10^{-6}° C^{-1} of alumina.

3.2.3. Aluminium–metal interdiffusion

The failure of many samples occurred at aluminium–metal interfaces, illustrating the importance of interdiffusion and growth of intermetallic layers. To gain some idea of the relative rates of these growth processes, 10 mm diameter all-metal samples were hot pressed using the main series normal conditions that had the material sequences Ni/Al/BS321/Al/BS431, Cu/Al/BS321/Al/BS310, Ti/Al/BS321/Al/Mo, Inconel 600/Al/BS321/Al/Invar. All these material combinations bonded and permitted cross-sectioning for interfacial characterization. Optical and electron microscopy revealed that intermetallic layers of very varying thicknesses had been formed as summarized in Table IV. The thickest two-zone layers were formed by copper but nickel and Invar also formed layers significantly thicker than those produced by the 18/9/1 CrNiTi steel BS321 used in this work. In contrast, titanium formed a very thin layer and molybdenum did not form any detectable intermetallic layer.

4. Discussion

The primary objective of this work was the identification of conditions that could be used to fabricate strong stainless steel–alumina joints using aluminium foil interlayers. For the present purpose a strong joint is one that can withstand a stress significantly greater than the 29.5 MPa produced by the "normal" conditions of a 50 MPa pressure applied for 30 min in an evacuated chamber at 590 to 600° C to a sample with 0.5 mm thick foil interlayers. Some success has been achieved, therefore, with the identification of two fabrication routes that produce joints with strengths of about 40 MPa and a post-fabrication technique that increases the strengths of normal samples to 50 to 70 MPa. To achieve the improved strength levels of 40 MPa the normal fabrication conditions were modified by either increasing the tempera-

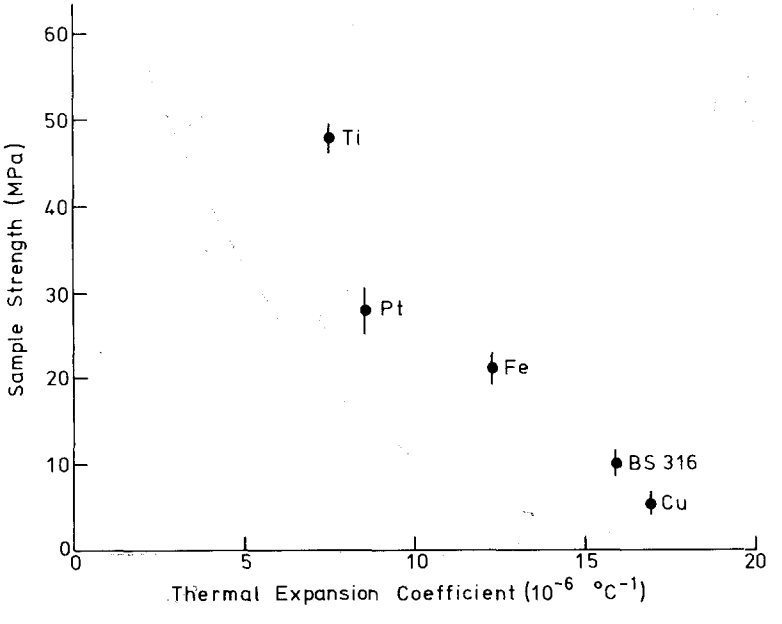

Figure 13 The strengths of truncated cone alumina–metal samples bonded with aluminium foils plotted as a function of the metal thermal expansion coefficients.

TABLE IV The compositions and thicknesses of intermetallic layers formed at metal–metal interfaces by bonding at 590–600° C for 30 min for

Couple	Intermetallic layer, composition	Thickness (μm)
BS321–Al	$(Fe_{0.71}Cr_{0.18}Ni_{0.07}Mn_{0.02}Si_{0.02})Al_{2.63}$	11.8
	$(Fe_{0.68}Cr_{0.16}Ni_{0.09}Mn_{0.02}Si_{0.05})Al_{3.25}$	8.8
BS310–Al	$(Fe_{0.54}Cr_{0.24}Ni_{0.19}Mn_{0.01}Si_{0.02})Al_{2.08}$	4
	$(Fe_{0.52}Cr_{0.25}Ni_{0.14}Mn_{0.01}Si_{0.08})Al_{3.15}$	4
BS431–Al	$(Fe_{0.81}Cr_{0.14}Ni_{0.03}Si_{0.02})Al_{3.12}$	10.5
Invar–Al	$(Fe_{0.62}Ni_{0.36}Cr_{0.01}Si_{0.01})Al_{3.01}$	20
	$(Fe_{0.50}Ni_{0.47}Si_{0.03})Al_{4.70}$	2
Ni–Al	$Ni\,Al_{1.71}$	10
	$Ni\,Al_{3.31}$	8
Cu–Al	$Cu\,Al_{1.08}$	17
	$Cu\,Al_{2.25}$	7
Ti–Al	$(Ti_{0.86}Si_{0.13}Fe_{0.01})Al_{1.69}$	1
Mo–Al	–	–
Inconel	$(Ni_{0.85}Fe_{0.11}Cr_{0.02}Si_{0.02})_2Al_{5.02}$	5
600–Al	$(Ni_{0.68}Cr_{0.19}Fe_{0.09}Si_{0.04})Al_{3.44}$	7

ture to 625° C or the foil thickness to 1.0 mm, while strengthening to 50 to 70 MPa was produced by post-fabrication heating to 100 to 150° C for 16 h.

Of these three methods for achieving stronger joints, the use of low-temperature stress-relieving post-fabrication heat treatments is considered to be least attractive because of its limited applicability. This procedure strengthened joints more than any other, but the benefit often may be empheral because of the weakening effects of stresses produced during cooling after themal excursions suffered by components in service or abnormal conditions. It seems probable that the high joint strengths of 50 to 70 MPa could be maintained only if the service conditions ensure that temperatures in excess of about 125° C are never experienced. There is little to choose between the other two methods of fabricating better quality joints, with strengths of 40 MPa. The decision as to which route is to be followed depends on the relative concern felt by a fabricator about the use of a temperature only 30 to 130° C below the iron–aluminium, nickel–aluminium and (iron, nickel)–aluminium eutectic melting points or the production of large flashes and component movement during fabrication that may render jigging difficult.

The results of the other experimental runs using less favourable conditions are also of some interest because they reveal the relative importance of a number of fabrication parameters and cast light on bonding mechanisms. Thus the data in Table III and various figures show that the bonding temperature and pressure are important parameters controlling the strengths of alumina–aluminium interfaces and suggest that the contact achieved by the initial deformation of the aluminimum foils represents a significant aspect of the quality of these interfaces. Whether this contact, and hence potential for bonding, can be enhanced by time-dependent diffusional processes cannot be deduced from the data because the samples that may have demonstrated this failed at their steel–aluminium interfaces, but the work of Heidt and Heimke [4] with aluminium– and copper–alumina, and of Klomp [5] with iron–alumina interfaces diffusion bonded at about 0.92 of the metal melting temperature in K (equivalent to 585° C for aluminium) shows that further strengthening can continue for a fraction of an hour.

The data presented in this paper also demonstrate the strengthening of alumina–aluminium interfaces by low-temperature stress-relieving anneals. The sensitivity of the strengths of such interfaces to stresses generated by thermal expansion mismatches is illustrated by the data plotted in Fig. 13, which suggest that truncated cone samples bonded in argon at 550° C would have fractured during cooling if the thermal expansion coefficient of the metal component had exceeded $20 \times 10^{-6}\ C^{-1}$. If a different type of sample had been used, the critical value of constraint on the free contraction of the bonded components will increase as the diameter of the bonded area becomes larger relative to the interlayer thickness. If the thermal expansion coefficients are a good match, the severity of the constraint-induced stressing will be slight, thus high-integrity accelerator modules with large joint areas have been

fabricated successfully using titanium electrodes bonded to alumina insulators [6].

The present work suggests that the strongest alumina–aluminium interfaces could be produced by bonding at 660° C, the melting point of aluminium, in an evacuated chamber. Equation 1 describes the strengths of alumina–aluminium–steel and predicts that they would have alumina–aluminium interfacial strengths of 68 MPa, while a similar analysis of alumina–aluminium sample data leads to a prediction of 83 MPa. These values appear to be realistic estimates of maximum strengths achievable with the sample geometry used in this work. Thus, Iseki and Nicholas [7] produced alumina–aluminium samples with complete interfacial contact by soldering truncated alumina cones together with aluminium foils at 1000° C, when aluminium wets the ceramic, and found room-temperature strengths of 68 ± 7 MPa when the interlayer thickness was 0.04 mm and 82 ± 7 MPa when it was 0.75 mm. Similarly, using a sessile drop geometry in which contraction stresses would have played a very minor role, Nicholas [8] observed room-temperature strengths of 91 to 92 MPa for alumina–aluminium interfaces produced at 700 to 900° C.

Even if a bonding procedure had been adopted which led to the achievement of these high alumina–aluminium interfacial strength levels, our work suggests that failure at stainless steel–aluminium interfaces would have prevented any benefit from being realized. Factors affecting the strengths of stainless steel–aluminium interfaces therefore are also of critical importance in determining joint quality and the data gathered in this study suggests that some of the most important of these factors are the fabrication time, temperature and environment. The thicknesses of the intermetallic layers formed at steel–aluminium interfaces increased with time and temperature in a manner that identified growth as being a diffusion-controlled process with an activation energy of about 227 kJ mol^{-1}. These growth data are in good accord with the results reported by Steinleitner [1] who also examined stainless steel–aluminium diffusion-bonded couples. Lower activation energies, 170 to 195 kJ mol^{-1}, than those observed in this work were reported by Denner and Jones [9] for the growth of aluminide layers on iron, but some difference might be expected because of the substantial proportions of chromium, nickel and other elements present in the

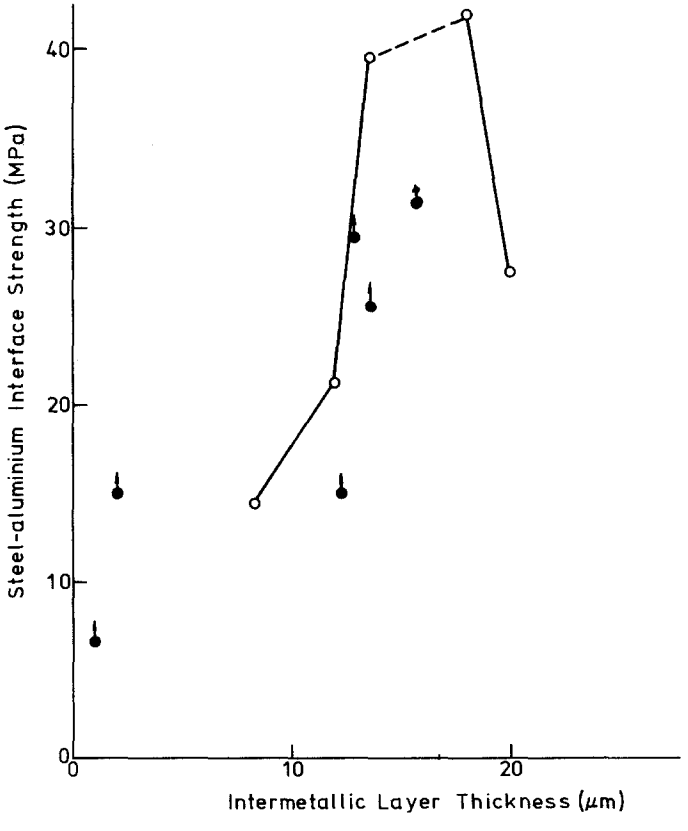

Figure 14 Sample strengths plotted as a function of the thicknesses of intermetallic layers formed at steel–alumina interfaces. Solid symbols indicate that failure occurred at alumina–aluminium interfaces and hence the steel–aluminium interface strengths are higher.

layers formed on stainless steel. Amongst these other elements, silicon is particularly noteworthy, because its concentration in the intermetallic layers was about ten times that in the stainless steel substrates and Layner and Kurakin [10] found that silicon retarded aluminide formation.

Table III provides some evidence that the growth of intermetallic layers was accompanied by changes in the strengths of the stainless steel–aluminium interfaces. The strengths of samples that failed at steel–aluminium interfaces at first increased as the intermetallic layers thickened but there is some evidence of a peak strength of about 40 MPa being associated with a layer thickness of 13 to 18 μm as shown in Fig. 14. Similar evidence of a peak interfacial strength, albeit at an intermetallic layer thickness of about 8 μm, was observed by Steinleitner [1] who subjected his samples to bending rather than tensile stresses. The reasons for these strength changes with intermetallic layer thickness have not been investigated, but they may be related to lattice mismatch effects between the fcc substrate and the complex monoclinic orthorhombic, and rhombohedral intermetallic layers. Regardless of the reason, Fig. 14 provides some guidance to the behaviour of stainless steel–aluminium interfaces and permits strength prediction to be made for samples bonded in an evacuated chamber on the basis of the intermetallic layer growth rates presented in Fig. 9.

The use of argon or air environments rather than a vacuum decreased the growth of intermetallic layers and weakened the stainless steel–aluminium interfaces of samples bonded at 600° C. This restriction of interdiffusion and bonding could be due to the influence of entrapped gas or oxide growth on the metal surfaces at high temperatures or both. It is not possible to be definite about the restriction mechanism, but the greater detrimental effect of air and the lack of that effect in samples bonded at 493° C suggests that the growth of oxide barriers was the more important factor.

The discussion has been concerned so far solely with the behaviour of alumina bonded to stainless steel by aluminium foil interlayers. However, the series of experiments using all metal samples demonstrated in passing that aluminium bonded readily to a fairly wide range of metals. Some of these, particularly copper, are probably unsuitable for joining to alumina because of the marked mismatch of thermal expansion coefficient and their readiness to form thick, and hence potentially flawed, intermetallic layers with aluminium. Other metals, particularly molybdenum and titanium, are better thermally matched to alumina and formed barely or not detectable intermetallic layers and therefore might be of use as bondable diffusion barriers between aluminium interlayers and reactive metal components. The interdiffusion behaviour of the other materials evaluated, BS310, BS431, Invar, Inconel 600 and nickel, resembled that of the BS321 stainless steel we used as a standard material not only in the thickness of intermetallic layers formed but also in their enrichment in silicon.

Finally, discussion of the data obtained during this study leads to speculation as to whether aluminium is the best interlayer material to use when bonding stainless steel to alumina. Aluminium has the advantage of bonding strongly to alumina at modest temperatures but its ability to form intermetallic layers with stainless steel is a disadvantage. Other ductile interlayer materials that might be considered include silver, gold, copper and nickel. These should form strong joints with the steel not accompanied by the growth of intermetallic layers. However, their ability to bond to alumina under conditions when complete contact is achieved is less than that of aluminium except in the case of nickel [8] and higher fabrication temperatures would have to be used which could increase the cost of the bonding process and cause softening of the steel components. Thus it is felt that the technique of using aluminium foil interlayers adopted in this study is a good candidate for optimization and development as a practical fabrication process for alumina–steel joints that do not have to withstand high temperatures.

Acknowledgements

The work described in this report was conducted as part of the Interface Technology Programme of the Harwell Metals and Chemicals Technology Centre with the financial support of the Engineering Materials Requirements Board of the Department of Industry. The work benefitted from the skills of Dr L. Welch who performed the EPMA studies, and discussions with Dr D. A. Mortimer.

References

1. G. STEINLEITNER, Proceedings of the D.V.S. Conference, "Fügen von Keramic, Glas und Metall",

Baden–Baden, December, 1980 (DVS (German Welding Society), Dusseldorf, 1981) p. 100.
2. C. F. OLD and M. G. NICHOLAS, unpublished work (1977).
3. W. DAWIHL and E. KLINGER, *Ber. Dtsch. Keram. Ges.* **46** (1969) 12.
4. G. HEIDT and G. HEIMKE, *ibid.* **50** (1973) 303.
5. J. KLOMP, *Sci. Ceram.* **5** (1970) 501.
6. T. JOY, "Development of high gradient, high vacuum accelerator tubes at Daresbury", 3rd International Conference on Electrostatic Technology, Oak Ridge, USA (1981). Daresbury Report DL/NUC/P132A.
7. T. ISEKI and M. G. NICHOLAS, *J. Mater. Sci.* **14** (1979) 687.
8. M. G. NICHOLAS, *ibid.* **3** (1968) 571.
9. S. G. DENNER and R. D. JONES, *Metals Technol.* **4** (1977) 167.
10. D. I. LAYNER and A. K. KURAKIN, *Fiz. Metal. Metalloved* **18** (1964) 146.

Received 15 April
and accepted 8 May 1982